Co-seismic surface deformation relating to the March 23, 2012 M_W 5.4 Ernabella (Pukatja) earthquake, central Australia

D. Clark, A. McPherson, T. I. Allen and M. De Kool

Minerals and Natural Hazards Division, Geoscience Australia
GPO Box 378, Canberra, ACT 2601, Australia
Email: Dan.Clark@ga.gov.au

1. INTRODUCTION

On 23 March 2012, at 09:25 GMT, a M_W 5.4 earthquake occurred in the eastern Musgrave Ranges region of north-central South Australia, near the community of Ernabella (Pukatja) (Fig. 1). This was the largest earthquake recorded on mainland Australia for 15 years, and the seventh historical earthquake sequence known to have produced a surface rupture in Australia. Numerous small communities in this remote part of central Australia reported the tremor, but there were no reports of injury or significant damage. The event resulted in the formation of a 1.6 km-long surface deformation zone comprising discontinuous reverse fault scarps with vertical displacements of more than 0.5 m, and extensive ground cracking.

The Ernabella earthquake occurred in non-extended Stable Continental Region (SCR - Johnston *et al.*, 1994) crust, in which fewer than fifteen historic earthquakes are documented to have produced co-seismic surface deformation (i.e. faulting or folding) worldwide (e.g. Gordon and Lewis, 1980; Lewis *et al.*, 1981; Bent, 1994; Seeber *et al.*, 1996; Van Arsdale, 2000; Rajendran *et al.*, 2001; Crone *et al.*, 2003; Dawson *et al.*, 2008, this study). Of these, only the Australian examples, the 1989 Ungava (Canada – Adams *et al.*, 1991, 1992; Bent *et al.*, 1994) and 1993 Killari (India - Rajendran *et al.*, 1996, 2000, 2001; Seeber *et al.*, 1996) earthquakes, have occurred in non-extended SCR crust (e.g. Schulte and Mooney, 2005) (Table 1). As such, the record of surface deformation resulting from the Ernabella earthquake provides an important constraint on models relating surface rupture length to earthquake magnitude (e.g. Johnston, 1994; Leonard, 2010), which are invaluable in the interpretation of Quaternary faulting in intraplate settings, such as Australia (e.g. Sandiford, 2003; Quigley *et al.*, 2006; Hillis *et al.*, 2008; Clark, 2010; Quigley *et al.*, 2010; Clark *et al.*, 2011, in press).

In this contribution we present seismic source parameters for the 23 March 2012 Ernabella event, place the event in its geologic context, and provide field evidence that verifies the occurrence of a surface rupture (herein called the Pukatja Scarp) relating to the earthquake.

© Commonwealth of Australia (Geoscience Australia) 2012.
This material is released under the **Creative Commons Attribution 3.0 Australia** Licence.
http://creativecommons.org/licenses/by/3.0/au/legalcode

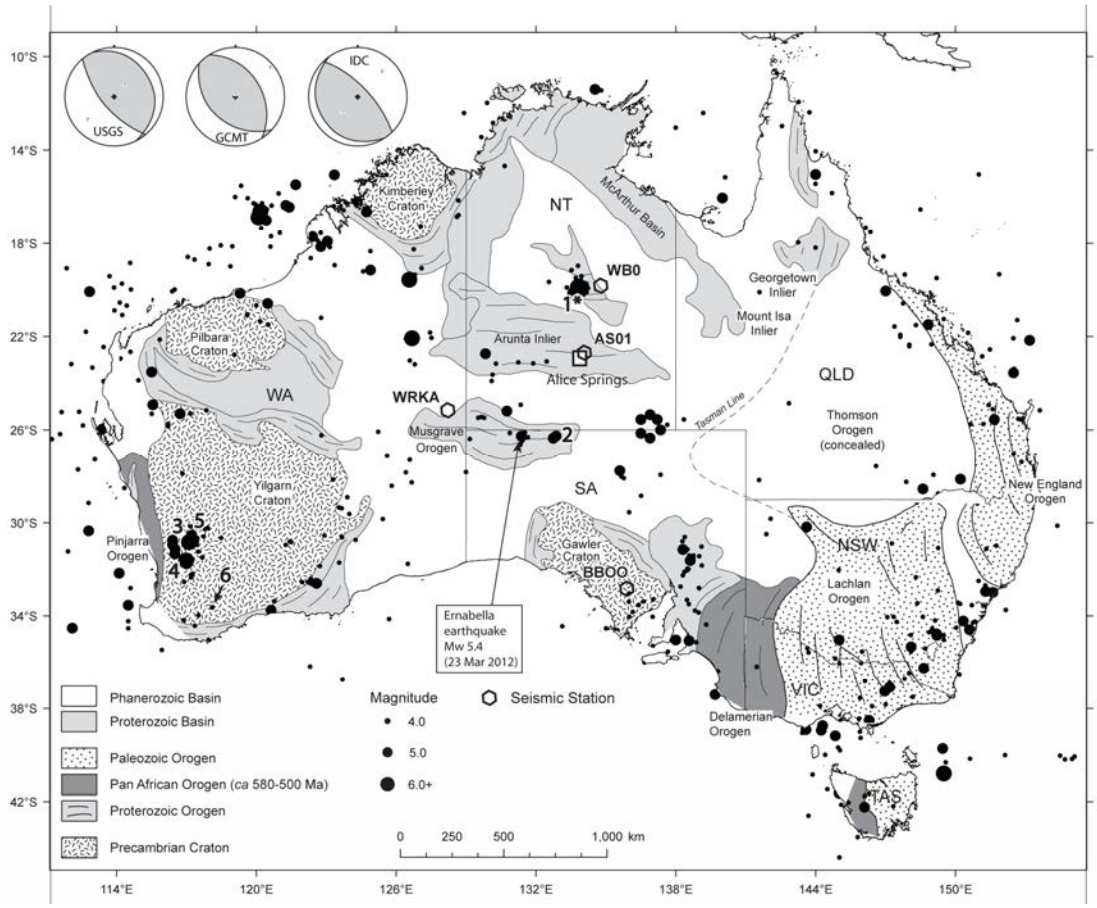

Figure 1. Distribution of basement rock provinces in Australia (modified after Allen *et al.* 2007). Epicentres for earthquakes larger than MW 4.0 are shown, including the location of the 23 March 2012 Ernabella earthquake. The locations of the six other historic earthquake sequences which resulted in surface rupture are also indicated: (1) Tennant Creek*, (2) Marryat Creek, (3) Cadoux, (4) Calingiri, (5) Meckering, (6) Katanning. *Tennant Creek consisted of a series of three M>6 events within 24 hours. Beachballs (top left) show focal mechanisms for the Ernabella earthquake computed by USGS, GCMT and IDC (cf. Table 2). Seismic stations shown are: AS01 – Alice Springs; BBOO – Buckleboo; WRKA – Warakurna; WB0 – Warramunga Array.

2. THE 23 MARCH 2012 ERNABELLA EARTHQUAKE

The M_W 5.4 (M_L 5.7) 23 March 2012 earthquake occurred in a remote location near Ernabella in northern South Australia. The earthquake occurred in an intraplate region approximately 70 km to the west of the location of the M_W 5.8 30 March 1986 Marryat Creek earthquake (Fig. 1; Table 1) (McCue *et al.*, 1987; McCue, 1990), which produced a 13 km long fault scarp (Machette *et al.*, 1993).

The M_W 5.4 Ernabella earthquake was recorded across the Australian National Seismic Network (ANSN) and stations operated by the South Australian government, in addition to other commercial and private stations. The nearest strong-motion recording was acquired some 400 km from the earthquake at Warakurna (WRKA – Fig. 1), Western Australia. The event was initially assigned a local magnitude M_L 6.1 by Geoscience Australia. Subsequent review of the local magnitude formula and station data resulted in the magnitude being recalculated and reduced to M_L 5.7 several days later.

Table 1. Surface rupture length (SRL), seismic moment (M_0) and moment magnitude (M_W) data for historic surface-rupturing earthquakes in non-extended SCR crust

Year/Event	SRL (km)	SRL range		M_0 (Nm)	M_0 range		M_W	M_W range		Reference	Original Reference
		min	max		min	max		min	max		
1968 Meckering	37	36	38	8.32E+18	6.1E+18	1.04E+19	6.58	6.49	6.64	Johnston *et al*. (1994)	Vogfjord & Langston (1987)
1970 Calingiri	3.3	3.3	3.3	1.738E+17	1.57E+17	1.92E+17	5.46#	5.43	5.49	Johnston *et al*. (1994)	Johnston *et al*. (1994)
1979 Cadoux	14	14	16	1.75E+18	1.25E+18	2.45E+18	6.13	6.03	6.23	Johnston *et al*. (1994)	Fredrich *et al*. (1988)
1986 Marryat Ck	13	13	13	5.13E+17	3.95E+17	6.67E+17	5.77	5.70	5.85	Johnston *et al*. (1994)	Fredrich *et al*. (1988)
1988 Tennant Ck (sum)*	36§	32	40	1.307E+19	1E+19	1.91E+19	6.71	6.63	6.82	Johnston *et al*. (1994)	Chung *et al*. (1992)
1989 Ungava, Canada	8.5	4.5	13	1.30E+18	9.00E+17	1.30E+18	6.00	5.80	6.20	Shulte & Mooney (2005)	Bent (1994)
1993 Killari Latur, India	3	1.0	3.0	1.80E+18	1.70E+18	2.20E+18	6.20	5.80	6.40	Shulte & Mooney (2005)	Seeber *et al*. 1996
2008 Katanning	1.26†	1.26	1.26	1.40E+16	1.35E+16	1.91E+16	4.73	4.72	4.82	Dawson *et al*. (2008)	Dawson *et al*. (2008)
2012 Ernabella	1.6	1.5	1.6	1.10E+17	1.00E+17	1.12E+17	5.33	5.30	5.33	this study	this study

Mw 5.46 ± 0.3 (derived by Johnston *et al*., 1994).

* Tennant Creek involved three surface rupturing events within a 24 hour period.

§ Includes 3 km rupture south of Western Lake Surprise scarp (Crone *et al*., 1992).

† derived from InSAR data.

The Ernabella earthquake was preceded by two foreshocks (M_L 3.8 and 4.3) in the two weeks beforehand. Only four small aftershocks (M_L 3.6-3.7) have been located by Geoscience Australia through to June 2012. Detailed analysis of the WRKA continuous data indicates 39 small aftershocks in the 24 hours following the main shock.

A number of organisations reported source parameters for the main shock (Table 2). Within uncertainty limits, almost all suggested a location approximately 20-30 km north of the remote community of Ernabella (Pukatja), approximately 320 km southwest of Alice Springs (Fig. 1). The sparse seismograph network in the source region resulted in poor depth constraints from standard location algorithms. Subsequent inspection of waveform data yielded little evidence of an obvious depth phase (David Jepsen, Geoscience Australia, pers. comm., June 2012), suggesting a shallow hypocentre.

Table 2. Source parameters for the 23 March 2012 Ernabella earthquake, as reported by several monitoring organizations. Values of M_W are derived from moment tensor solutions.

Organization	Time (GMT)	Lat	Lon	Depth (km)	M_W	M_L	m_b	M_S
Geoscience Australia (GA)	09:25:14	-26.16	131.95	4.0 (0*)	5.4	5.7	-	5.5
US Geological Survey (USGS)	09:25:16	-26.06	132.12	11.0	5.3	-	5.6	5.3
Global Centroid Moment Tensor (GCMT)	09:25:18	-26.11	132.08	12.0	5.3	-	5.6	-
St. Louis University (SLU)	09:25:16	-26.07	132.12	20.0	5.3	-	-	-

* Officially reported depth from the Australian National Seismic Network.

Table 3. Moment tensor parameters for the 23 March 2012 Ernabella, South Australia, earthquake from several monitoring organisations. The strike, dip and rake of each nodal plane (NP1 and NP2) are represented in units of degrees.

Organisation	NP1			NP2		
	Strike	Dip	Rake	Strike	Dip	Rake
Global Centroid Moment Tensor (GCMT)	143	45	95	316	45	85
Geoscience Australia (GA)	136	72	87	327	17	100
St. Louis University (RMT)	140	70	85	334	21	103

A moment tensor and depth for the event were derived by fitting the spectra of the associated surface waves observed at 21 stations of the ANSN (Table 3). Synthetics were generated using the modal summation method from the "Computer Programs in Seismology" package (Herrmann, 2002), and the local earth and dispersion models were taken from the CUB global shear velocity model (Shapiro and Ritzwoller, 2002). Results were compared with other focal mechanisms for the event from the Global Centroid Moment Tensor (CMT) database (e.g. Ekström *et al.*, 2012), and St. Louis University's Regional Moment Tensor (RMT) (e.g. Herrmann *et al.*, 2008, 2011). The focal mechanism solutions (Fig. 1) are generally consistent, indicating reverse displacement along a southeast striking failure plane. In addition, the *P*-axis orientations are consistent with the modelled NE-SW trending compressive crustal stress field (Hillis and Reynolds, 2000, 2003). Table 2 shows a range of reported

hypocentral depth estimates between 4 and 20 km. Such a discrepancy is not unexpected given the different methods, data sets and earth models used in the quoted solutions, and the fact that surface wave spectra are more sensitive to focal mechanism than to depth. Systematic effects due to model assumptions and uncertainties in the earth models make it very difficult to attach a formal significance to the difference between models and observed spectra. Therefore we adhere to standard practice and only quote our best-fitting solution without formal errors.

3. GEOLOGICAL SETTING

The geology of the Australian continental crust west of the Tasman Line (Fig. 1) (Direen and Crawford, 2003) is characterized by tectonically stable cratonic nuclei (typically of Archaean and Palaeoproterozoic age) that are bounded by polycyclic orogenic belts (dominantly Mesoproterozoic and younger - e.g. Shaw *et al.*, 1996; Fitzsimons, 2000; Karlstrom *et al.*, 2001; Betts *et al.*, 2002; Betts and Giles, 2006; Wade *et al.*, 2006).

The Ernabella earthquake occurred in the eastern Musgrave Province, one of the orogenic belts found in central Australia (Fig. 1). The province preserves deformation structures, high-grade metamorphic rocks and magmatic suites ranging in age from Mesoproterozoic to early Cambrian (Camacho and McDougall, 2000; Edgoose *et al.*, 2004; Raimondo *et al.*, 2010) (Fig. 2). The province is divided into two subdomains based on variation in metamorphic grade across the crustal-scale *ca.* 550 Ma Woodroffe Thrust (Fig. 2); Fregon and Mulga Park. The Fregon Subdomain, within the hanging wall of the 30° southeast-dipping Woodroffe Thrust, preserves the upper-amphibolite to granulite facies Birksgate Complex (Lambeck and Burgess, 1992; Camacho *et al.*, 1995; Camacho and McDougall, 2000; Aitken and Betts, 2009). The surface trace of the Woodroffe Thrust occurs as a 1.5 km wide mylonitized shear zone (Lin *et al.*, 2005) approximately 10 km to the north and northwest of the Pukatja Scarp (Fig. 2 - inset). For clarity, an epicentral depth of 4–5 km places the Ernabella event *within* the hanging wall of the Woodroffe Thrust, the fault plane of which would be at approximately 9 km depth.

4. SURFACE DEFORMATION

Surface deformation related to the 23 March 2012 Ernabella earthquake was investigated in the field from 4–5 April 2012. A 1.6 km long arcuate deformation zone, comprising southwest-side up scarp sections and linking and terminal fractures, was identified crossing an extremely low relief (< 3 m), near level (< 1% slope) sand plain. The sand plain comprises colluvial, fluvial and sheetwash landscape elements (Fig. 3). The western half of the feature trends roughly east-west and occurs along strike from a prominent lithological contact between charnockitic granitoids of the Ernabella Batholith and Birksgate Complex gneisses (Edgoose *et al.*, 2004; Aitken and Betts, 2009) (Figs. 2 and 3). This contact dips 30° towards the southwest, and is obscured by sand plain deposits ~200 m east of the scarp trace. Surface expression of the scarp is typically in the form of 'mole-tracks' (e.g. Lin *et al.*, 2004), where a thin surface crust (1-5 cm thick) has been broken into 'A-tent' forms. Vertical displacements along this western limb are in most places less than 0.1 m (Figs. 3 and 4a).

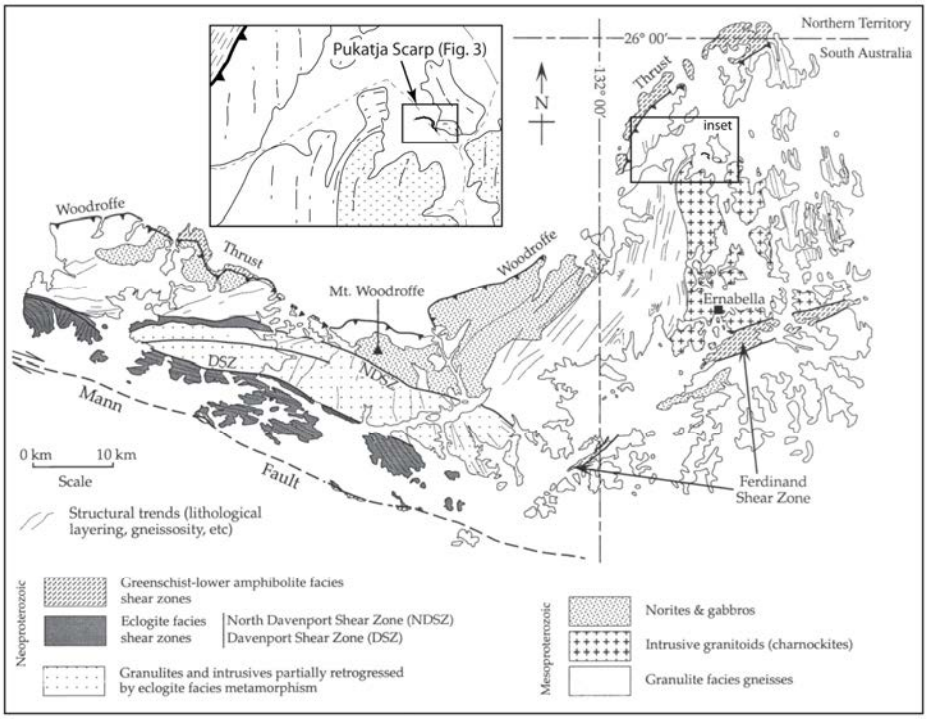

Figure 2. Generalised geological map of the eastern Musgrave Ranges, South Australia (after Camacho and McDougall, 2000), showing the location of the Pukatja Scarp. Rocks stratigraphically below the Woodroffe Thrust (i.e. to the north) are collectively known as the Mulga Park Subdomain; the Fregon Subdomain is located within the hanging wall of the Woodroffe Thrust. Inset (Fig. 3) shows details of geology in the local area around the surface rupture, highlighting the proximity of the scarp to a major lithological boundary.

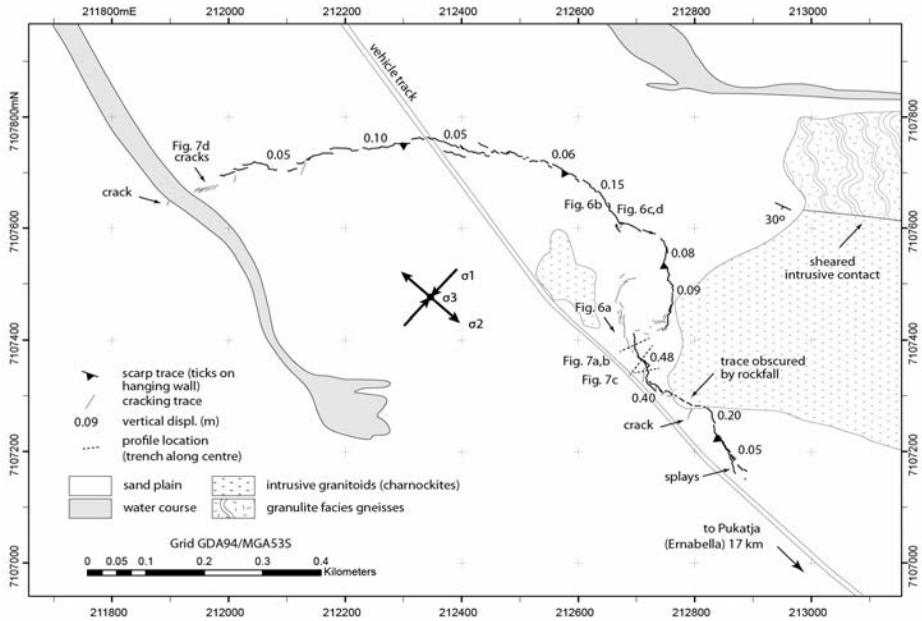

Figure 3. Mapped surface trace of the Pukatja Scarp showing ground surface displacement (black lines), tension cracks (grey lines) and measured vertical displacement. Arrows in the centre of the figure indicate principal stress orientations. Topographic profiles denoted by dotted black lines and labelled with related figure numbers. NOTE: the hand trench excavated across the scarp is co-located with the middle topographic profile.

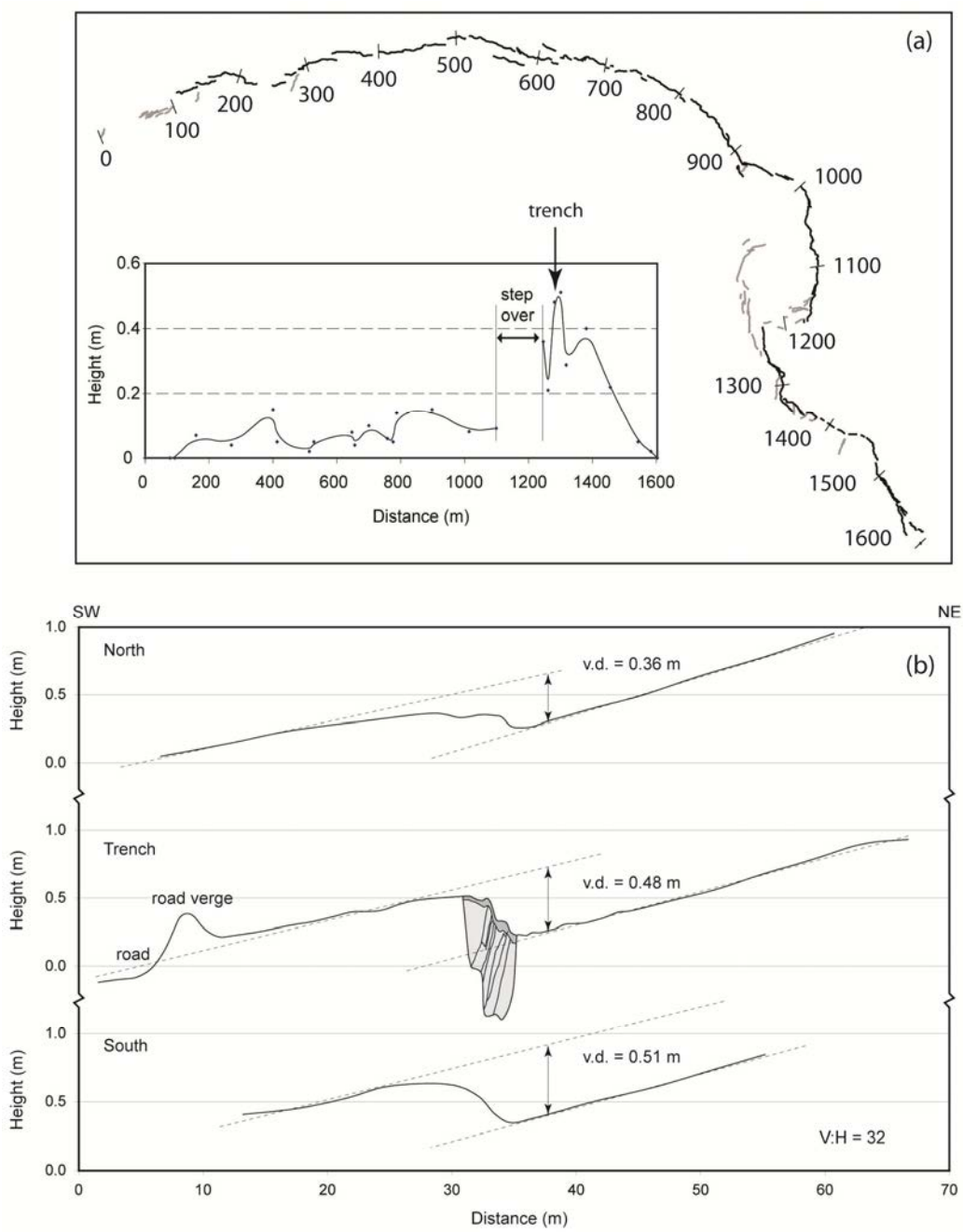

Figure 4. Surveyed topographic data for the Pukatja Scarp. (a) Plot of distance along the scarp versus vertical displacement with smoothed trendline. Scarp line symbology as for Figure 3. (b) Topographic profiles across the Pukatja Scarp in the region of maximum vertical displacement (v.d.). See Figure 3 for traverse locations – middle profile traverses the trench excavated on the scarp.

Cracking patterns between left-stepping scarp segments in the western 700 m of the scarp show little evidence for a consistent sense of lateral shear, despite the expectation of a sinistral component to the slip. Measured crack and fissure orientations along the entire length of the scarp (Fig. 5) are consistent with the *P*-axis orientations inferred from the focal mechanisms, indicating that the scarp formed in response to NE-oriented horizontal compression.

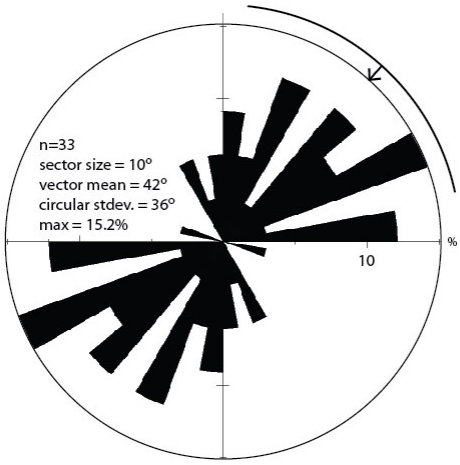

Figure 5. Rose diagram showing orientations of cracks across which no vertical motion was apparent.

Beyond 700 m from the western end of the scarp, vertical displacements increase as the orientation of the scarp turns to the southeast (Fig. 4a), grossly perpendicular to the *P*-axis of the focal mechanisms (cf. Fig. 1). The surface expression is a pressure-ridge form (Fig. 6c), often characterised by multiple steps (implying multiple slip surfaces – Fig. 6a) and occasional backthrust elements (Fig. 6b). More northerly trending scarp segments exhibit prominent shear fractures on the pressure ridge face consistent with a dextral component to the slip (Fig. 6d).

Approximately 300 m from its south-eastern end, the scarp exhibits a prominent step to the east (away from the track) (Fig. 3). The deformation zone between scarp segments, which is some 55 m wide, contains a high density of easterly to north-easterly trending tension fissures and cracks. Individual fissures may extend for ten metres or more and be up to 0.1 m wide. A semi-continuous fissure system also extends north from the tip of the westerly scarp segment before turning to the east-northeast and terminating. It is possible that the northerly trending section of this feature, which is broadly scarp-parallel, relates to differential motion between the soil mantle and underlying bedrock during ground shaking.

The maximum vertical displacements of 0.36–0.51 m (Fig. 4a, b) occur in the 300 m south of the prominent right step in the scarp trace (Fig. 6a). The scarp face in this section is marked by the presence of a 1–2 m wide zone of dead grasses; their roots having been torn by the ground deformation. A small (3.0 m × 1.2 m × 0.9 m) hand trench excavated across the scarp (Fig. 7) where the vertical displacement was measured to be 0.48 m (Fig. 4b) revealed evidence for multiple slip planes dipping shallowly (25 ± 3°) to the southwest (Figs. 7 and 8a). At this location the scarp is oriented perpendicular to the inferred compression axis, and no evidence for strike-slip motion was observed (Fig. 8b).

Figure 6. Field photographs along the Pukatja Scarp. (a) View south along the scarp at point of maximum vertical displacement (shown by arrow). Note that grass has been killed in a 2 m wide strip along the scarp face. Trench location is near the tree in the mid ground (212700mE/7107379mN); (b) Small backthrust splay. The main deformation front jumps to the location of the backthrust trace beyond the geologist. Note tension fractures in the right hand branch, consistent with a component of dextral slip (see also (d)); view is to the south. (212653mE/7107638mN); (c) Scarp displacing a previously level sand plain. Photo taken looking north; note book is 130 mm high (212654mE/7107632mN); (d) Small-scale right steps in the scarp trace and associated tension fractures indicating minor dextral displacement associated with dominant thrust displacement. Photo taken looking west; tape measure is 0.5 m long (212654mE/7107632mN). Coordinates in GDA94/MGA53.

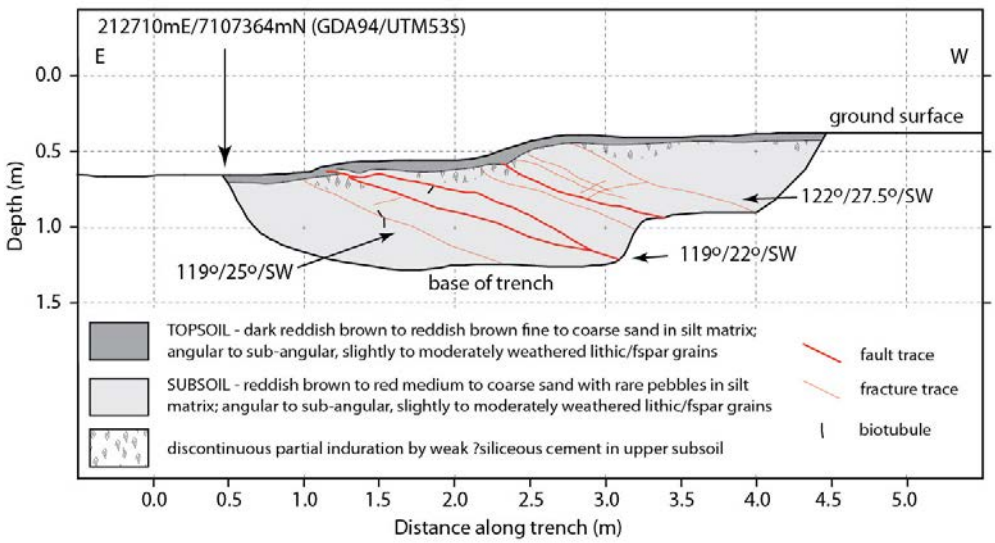

Figure 7. Trench log of the southern wall excavated over the Pukatja Scarp showing shallowly (25 ± 3°) southwest-dipping reverse faults displacing the ground surface.

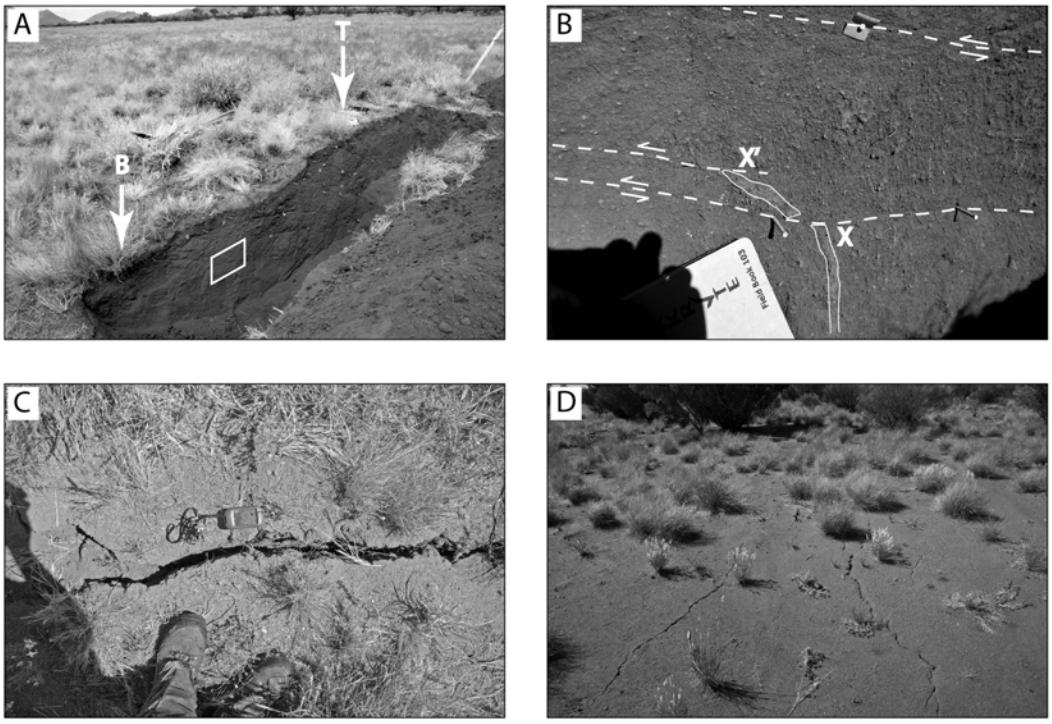

Figure 8. (a) Hand trench excavated through Pukatja Scarp. Shear planes dip shallowly to the right (southwest) at 25±3º. Note dead grasses along the face of the scarp between top (T) and bottom (B) marks, which have had their roots torn by the rupture. Trench is 3 m long. White box indicates location of Figure 8b. View to the south (212710mE/7107364mN); (b) Detail of southern trench wall showing a vertical biotubule displaced to the top left by shearing. Total shear recorded by the feature, between points X and X', is 83 mm. The existence of the biotubule above the shear marked by nails suggests minimum strike slip motion at this site; (c) Vertical tension fissure trending ~17° east of north. GPS is 125 mm wide (212712mE/7107347mN); (d) Bifurcating cracks at western terminus of the scarp. Cracks are up to 20 mm wide and show no vertical displacement. (211967mE/7107674mN). Coordinates in GDA94/MGA53.

North-easterly oriented tension fissures are most prominently developed between the trench and where the scarp traverses a bedrock spur (cf. Fig. 3). Here fissures exhibit a dilatancy of 0.4–0.5 m (Fig. 8c). South of the bedrock spur the vertical displacement decreases rapidly and the scarp terminates in a series of bifurcating synthetic splays (Figs. 3 and 4a). In contrast, the western end of the scarp terminates in a horsetail splay of divergent fissures (Fig. 8d; cf. Fig. 3). These fissures are developed in the dilatant quadrant with respect to the focal mechanisms and crack orientations, indicating a component of sinistral lateral motion on the western arm of the scarp.

The observation of terminal structures at both ends of the scarp (cf. Kim *et al.*, 2004) provides confidence that the full extent of surface deformation relating to the Ernabella earthquake has been mapped. No indication was found for previous surface rupture at this location, either in the landscape, or in the walls of the trench. However, the nature of the sediment exposed in the trench walls (i.e. angular feldspar grains, minimal soil development – Fig. 7) suggests that the land surface is relatively young (perhaps in the order of a few thousands of years old), potentially post-dating any previous surface-rupturing event, should one have occurred. Thunderstorms on the 4th and 5th of April significantly degraded the fine detail of the current surface

expression of the scarp. It might be expected that much of the scarp will be unrecognisable within months of the earthquake's occurrence.

5. DISCUSSION

The orientation of the *P*-axes from the focal mechanisms (Fig. 1) and the orientation of tension cracks associated with scarp sections (Fig. 5) are consistent with the northeast-trending horizontal crustal compressive stress inferred from the 1986 Marryat Creek (McCue *et al.*, 1987) and 1988 Tennant Creek earthquake events (Bowman, 1988; Choy and Bowman, 1990; Bowman, 1992). It is also consistent with modelling based upon focal mechanisms for the above events, and further supported by *in situ* stress data for the Australian crust (e.g. Hillis and Reynolds, 2003). The failure planes exposed in the trench excavated across the Pukatja Scarp (Fig. 6) are consistent with the southwest-dipping nodal planes of the focal mechanisms derived for the earthquake (Fig. 1); these are therefore preferred as the fault plane. The curvilinear lithological contact coincident with the E–W trending, low-displacement northern rupture segment appears to have been coincident with termination of the NW-trending rupture, which by implication nucleated near the southern end of the scarp.

The slip distribution and rupture geometry for Australian earthquakes is poorly understood, and attempts to model it have required numerous assumptions and involved significant simplifications (e.g. Somerville *et al.,* 2010). Leonard (2010) proposed that the width (W) of reverse fault ruptures scale proportionally to length (L) as $L^{2/3}$. Applying this to the seismic moment, M_0, for the Ernabella earthquake (~1.1 $\times 10^{17}$ Nm) indicates that the rupture dimensions could be in the order of 3.8 (L) $\times$ 3.3 (W) km. Standard relations (e.g. Johnston, 1994; Wells and Coppersmith, 1994; Leonard, 2010) suggest that an event of this moment might be associated with an average slip of approximately 0.3 m, equivalent to an average uplift of 0.13–0.16 m across a 25–30° dipping fault plane. Such an uplift value is broadly consistent with the average observed along the Pukatja Scarp, given that maximum slip can be 2–2.5 times the average slip (Wells and Coppersmith, 1994; Hemphill-Haley and Weldon, 1999). The modest width of the rupture suggests that several kilometres separate the base of the rupture from the underlying Woodroffe Thrust (e.g. Camacho *et al.*, 1995).

ACKNOWLEDGEMENTS

We are extremely grateful to the people of the Anangu Pitjantjatjara Yankunytjatjara community of central Australia who, at short notice, kindly granted permission for us to access and work on their land. In particular, we thank Peter Nyaningu, in whose homeland the surface rupture was located, and Peter Ruwoldt, whose curiosity and willingness to share his observations and images of the ground cracking provided the impetus to initiate this work. Bob Herrmann is thanked for rapid provision of his Regional Moment Tensor (RMT) solution for the Ernabella earthquake, and subsequent support to the authors in configuring his RMT code for Australia. Many thanks also to Hugh Glanville, who extracted the aftershock data, and to two internal reviewers whose comments improved the manuscript. This paper is published with the permission of the Chief Executive Officer of Geoscience Australia.

REFERENCES

Adams, J., Percival, J., Wetmiller, R., Drysdale, J. and Robertson, P. (1992). Geological controls on the 1989 Ungava surface rupture a preliminary interpretation, *Geological Survey of Canada Paper* **92C**, 147155.

Adams, J., Wetmiller, R., Hasegawa, H. and Drysdale, J. (1991). The first surface faulting from a historical earthquake in North America. *Nature* **352**, 617-619.

Aitken, A. R. A. and Betts, P. G. (2009). Multi-scale integrated structural and aeromagnetic analysis to guide tectonic models: An example from the eastern Musgrave Province, Central Australia. *Tectonophysics* **476**, 418-435.

Allen, T. I., Cummins, P. R., Dhu, T. and Schneider, J. F. (2007). Attenuation of ground-motion spectral amplitudes in southeastern Australia. *Bulletin of the Seismological Society of America* **97**, 1279–1292.

Bent, A. L. (1994). The 1989 (Ms 6.3) Ungava, Quebec, Earthquake: a Complex Intraplate Event. *Bulletin of the Seismological Society of America* **84**, 1075-1088.

Betts, P. G. and Giles, D. (2006). The 1800–1100 Ma tectonic evolution of Australia. *Precambrian Research* **144**, 92-125.

Betts, P. G., Giles, D., Lister, G. S. and Frick, L. R. (2002). Evolution of the Australian lithosphere. *Australian Journal of Earth Sciences* **49**, 661-695.

Bowman, J. R. (1988). Constraints on locations of large intraplate earthquakes in the Northern Territory, Australia from observations at the Warramunga seismic array. *Geophysical Research Letters* **15**, 1475-1478.

Bowman, J. R. (1992). The 1988 Tennant Creek, Northern Territory, earthquakes: a synthesis. *Australian Journal of Earth Sciences* **39**, 651-669.

Camacho, A. and McDougall, I. (2000). Intracratonic, strike-slip partitioned transpression and the formation and exhumation of eclogite facies rocks: An example from the Musgrave Block, central Australia. *Tectonics* **19**, 978-996.

Camacho, A., Vernon, R. H. and Fitzgerald, J. D. (1995). Large volumes of anhydrous pseudotachylyte in the Woodroffe Thrust, eastern Musgrave Ranges, Australia. *Journal of Structural Geology* **17**, 371- 383.

Choy, G. L. and Bowman, J. R. (1990). Rupture process of a multiple main shock sequence; analysis of teleseismic, local, and field observations of the Tennant Creek, Australia, earthquakes of January 22, 1988. *Journal of Geophysical Research, B, Solid Earth and Planets* **95**, 6867-6882.

Chung, W.-Y., Johnston, A. C. and Pujol, J. 1992. *A global study of stable continental intraplate earthquakes: focal mechanisms, source-scaling relations, and*

seismotectonics. Final Report, EPRI RP-2556-54, Electric Power Research Institute, Palo Alto, California, 252 p.

Clark, D. (2010). Identification of Quaternary scarps in southwest and central west Western Australia using DEM-based hill shading: application to seismic hazard assessment and neotectonics. *International Journal of Remote Sensing* **31**, 6297-6325.

Clark, D., McPherson, A. and Collins, C. D. N. (2011). Australia's seismogenic neotectonic record: a case for heterogeneous intraplate deformation. *Geoscience Australia Record* **2011/11**, 95 p.

Clark, D., McPherson, A. and Van Dissen, R. (in press). Long-term behaviour of Australian Stable Continental Region (SCR) faults. *Tectonophysics*.

Crone, A. J., de Martini, P. M., Machette, M. N., Okumura, K. and Prescott, J. R. (2003). Paleoseismicity of two historically quiescent faults in Australia: implications for fault behavior in Stable Continental Regions. *Bulletin of the Seismological Society of America* **93**, 1913-1934.

Crone, A. J., Machette, M. N. and Bowman, J. R. (1992). Geologic investigations of the 1988 Tennant Creek, Australia, earthquakes - implications for paleoseismicity in stable continental regions. *United States Geological Survey Bulletin* **2032-A**, 51 p.

Dawson, J., Cummins, P., Tregoning, P. and Leonard, M. (2008). Shallow intraplate earthquakes in Western Australia observed by Interferometric Synthetic Aperture Radar. *Journal of Geophysical Research* **113**, doi:10.1029/2008JB005807.

Direen, N. G. and Crawford, A. J. 2003. The Tasman Line: where is it, what is it, and is it Australia's Rodinian breakup boundary? *Australian Journal of Earth Sciences* **50**, 491-502.

Edgoose, C. J., Scrimgeour, I. R. and Close, D. F. (2004). Geology of the Musgrave Block, Northern Territory. *Northern Territory Geological Survey Report* **15**.

Ekström, G., Nettles, M. and Dziewonski, A. M. (2012). The global CMT project 2004-2010: Centroid-moment tensors for 13,017 earthquakes. *Physics of the Earth and Planetary Interiors* **200-201,** 1-9.

Fitzsimons, I. C. W. (2000). A review of tectonic events in the East Antarctic Shield and their implications for Gondwana and earlier supercontinents. *Journal of African Earth Sciences* **31**, 3-23.

Fredrich, J., McCaffrey, R. and Denham, D. 1988. Source parameters of seven large Australian earthquakes determined by body waveform inversion. *Geophysical Journal* **95**, 1-13.

Gordon, F. R. and Lewis, J. D. (1980). The Meckering and Calingiri earthquakes October 1968 and March 1970. *Western Australia Geological Survey Bulletin* **126**, 229 p.

Hemphill-Haley, M. A. and Weldon, R. J. (1999). Estimating prehistoric earthquake magnitude from point measurements of surface rupture. *Bulletin of the Seismological Society of America* **89**, 1264-1279.

Herrmann, R. B. (ed.) (2002). *Computer Programs in Seismology: an overview of synthetic seismogram computation (Version 3.30)* [Computer Software]. Saint Louis University, St. Louis, MI.

Herrmann, R. B., Benz, H. and Ammon, C. J. (2011). Monitoring the earthquake source process in North America. *Bulletin of the Seismological Society of America* **101**, 2609-2625.

Herrmann, R. B., Withers, M. and Benz, H. (2008). The April 18, 2008 Illinois earthquake: An ANSS monitoring success. *Seismological Research Letters* **79**, 830-843.

Hillis, R. R. and Reynolds, S. D. (2000). The Australian stress map. *Journal of the Geological Society of London* **157**, 915-921.

Hillis, R. R. and Reynolds, S. D. (2003). In situ stress field of Australia. *In*: R. R. Hillis and D. Müller (Eds.), Evolution and dynamics of the Australian Plate. *Geological Society of Australia Special Publication* **22**, pp. 49-58.

Hillis, R.R., Sandiford, M., Reynolds, S.D., Quigley, M.C., 2008. Present-day stresses, seismicity and Neogene-to-Recent tectonics of Australia's 'passive' margins: intraplate deformation controlled by plate boundary forces. *In*: H. Johnson, A. G. Doré, R. W. Gatliff, R. Holdsworth, E. R. Lundin and J. D. Ritchie (Eds.), The Nature and Origin of Compression in Passive Margins. *Geological Society of London Special Publication* **306**. pp. 71-90.

Johnston, A. C. (1994). Seismotectonic interpretations and conclusions from the stable continental region seismicity database. *In*: A. C. Johnston, K. J. Coppersmith, L. R. Kanter and C. A. Cornell (Eds.), The earthquakes of stable continental regions-v. 1, Assessment of large earthquake potential. *Electric Power Research Institute Report* **4-1-4-103**. Palo Alto, California.

Johnston, A. C., Coppersmith, K. J. Kanter, L. R. and Cornell, C. A. (1994). The earthquakes of stable continental regions. *Electric Power Research Institute Report* **TR102261V1**. Palo Alto, California.

Karlstrom, K. E., Åhäll, K.-I., Harlan, S. S., Williams, M. L., McLelland, J. and Geissman, J. W. (2001). Long-Lived (1.8-1.0 Ga) convergent orogen in southern Laurentia, its extensions to Australia and Baltica, and implications for refining Rodinia. *Precambrian Research* **111**, 5-30.

Kim, Y.-S., Peacock, D. C. P. and Sanderson, D. J. (2004). Fault damage zones. *Journal of Structural Geology* **26**, 503-517.

Lambeck, K. and Burgess, G. (1992). Deep crustal structure of the Musgrave Block, central Australia: results from teleseismic travel time anomalies. *Australian Journal of Earth Sciences* **39**, 1–19.

Leonard, M. (2010). Earthquake fault scaling: relating rupture length, width, average displacement, and moment release. *Bulletin of the Seismological Society of America* **100**, 1971-1988.

Lewis, J. D., Daetwyler, N. A., Bunting, J. A. and Moncrieff, J. S. (1981). The Cadoux earthquake. *Western Australia, Geological Survey Report* **1981/11**, 133 p.

Lin, A., Guo, J. and Fu, B. (2004). Co-seismic mole track structures produced by the 2001 Ms 8.1 Central Kunlun earthquake, China. *Journal of Structural Geology* **26**, 1511-1519.

Lin, A., Maruyama, T., Aaron, S., Michibayashi, K., Camacho, A. and Kano, K. (2005). Propagation of seismic slip from brittle to ductile crust: Evidence from pseudotachylyte of the Woodroffe thrust, central Australia. *Tectonophysics* **402**, 21-35.

Machette, M. N., Crone, A. J. and Bowman, J. R. (1993). Geologic investigations of the 1986 Marryat Creek, Australia, earthquake - implications for paleoseismicity in stable continental regions. *USGS Bulletin* **2032-B**, 29 p.

McCue, K. (1990). Australia's large earthquakes and Recent fault scarps. *Journal of Structural Geology* **12**, 761-766.

McCue, K. F., Barlow, B. C., Denham, D., Jones, T., Gibson, G. and Michael-Leiba, M. O. (1987). Another chip off the old Australian block. *Eos, Transactions, American Geophysical Union* **68**, 609-612.

Quigley, M., Clark, D. and Sandiford, M. (2010). Late Cenozoic tectonic geomorphology of Australia. *Geological Society of London Special Publication* **346**, 243-265.

Quigley, M. C., Cupper, M. L. and Sandiford, M. (2006). Quaternary faults of south-central Australia: palaeoseismicity, slip rates and origin. *Australian Journal of Earth Sciences* **53**, 285-301.

Raimondo, T., Collins, A. S., Hand, M., Walker-Hallam, A., Smithies, R. H., Evins, P. M. and Howard. H. M. (2010). The anatomy of a deep intracontinental orogen. *Tectonics* **29**, TC4024.

Rajendran, C. P. (2000). Using geological data for earthquake studies: A perspective from peninsular India. *Current Science* **79**, 1251-1258.

Rajendran, C. P., Rajendran, K. and John, B. (1996). The 1993 Killari (Latur), central India, earthquake: an example of fault reactivation in the Precambrian crust. *Geology* **24**, 651-654.

Rajendran, K., Rajendran, C. P., Thakkar, M. and Tuttle, M. P. (2001). The 2001 Kutch (Bhuj) earthquake: Coseismic surface features and their significance. *Current Science* **80**, 1397-1405.

Sandiford, M. (2003). Neotectonics of southeastern Australia: linking the Quaternary faulting record with seismicity and in situ stress. *In*: R. R. Hillis and D. Müller (Eds.), Evolution and dynamics of the Australian Plate. *Geological Society of Australia Special Publication* **22**, pp. 101-113.

Schulte, S. M. and Mooney, W. D. (2005). An updated global earthquake catalogue for stable continental regions: reassessing the correlation with ancient rifts. *Geophysical Journal International* **161**, 707-721.

Seeber, L., Ekstrom, G., Jain, S. K., Murty, C. V. R., Chandak, N. and Armbruster, J. G. (1996). The 1993 Killari earthquake in central India: A new fault in Mesozoic basalt flows? *Journal of Geophysical Research* **101**, 8543-8560.

Shapiro, N. M. and Ritzwoller, M. H. (2002). Monte-Carlo inversion for a global shear velocity model of the crust and upper mantle. *Geophysical Journal International* **151**, 88-105.

Shaw, R. D., Wellman, P., Gunn, P. J., Whitaker, A. J., Tarlowski, C. and Morse, M. (1996). Guide to using the Australian crustal elements map. *Australian Geological Survey Organisation Record* **1996/30**, 93 p.

Somerville, P., Graves, R. W., Collins, N. F., Song, S. G. and Ni, S. (2010). *Ground motion models for Australian earthquakes*. Final report to Geoscience Australia, 30 March 2010. URS Corporation, Pasadena, CA.

Van Arsdale, R. (2000). Displacement history and slip rate on the Reelfoot Fault of the New Madrid Seismic Zone. *Engineering Geology* **55**, 219-226.

Vogfjörd, K. S. and Langston, C. A. (1987). The Meckering earthquake of 14th October 1968: a possible downward propagating rupture. *Bulletin of the Seismological Society of America* **77**, 1558-1578.

Wade, B. P., Barovich, K. M., Hand, M., Scrimgeour, I. R. and Close, D. F. (2006). Evidence for Early Mesoproterozoic Arc Magmatism in the Musgrave Block, Central Australia: Implications for Proterozoic Crustal Growth and Tectonic Reconstructions of Australia. *The Journal of Geology* **114**, 43-63.

Wells, D. L. and Coppersmith, K. J. (1994). New empirical relationships among magnitude, rupture length, rupture width, rupture area, and surface displacement. *Bulletin of the Seismological Society of America* **84**, 974-1002.